Observations of confined fast ions in MAST-U with the Neutron Camera Upgrade

M. Cecconello[1,2], I. Dolby[1], A. Sperduti[2], S. J. Holm[2], A. Hjalmarsson[2], G. Ericsson[2], I. Fitzgerald[3], S. Y. Allan[3], J. Voller[3], B. Honey[3], B. A. Nizar[3], S. D. Elmore[3], and the MAST-U team*

[1] Department of Physics, Durham University, DH1 3LE, UK [2] Department of Physics and Astronomy, Uppsala University, Uppsala, Sweden
[3] UKAEA, CCFE Culham Science Centre, Abingdon, Oxon, OX14 3DB, UK * See author list of J. Harrison, et al. 2019 Nucl. Fusion 59 11201

Introduction

MAST-U is highly suited to the study of the interactions between Fast Ions (FIs) and MHD instabilities. During the first MAST-U campaign MU01, the **Neutron Camera Upgrade** (NCU) was one FI diagnostic used to observe the behaviour of confined FIs during various plasma instabilities, such as:
-- TAEs
-- Sawteeth
-- Fishbones
-- NTMs,
as well as observing and comparing the effect of on-axis vs off-axis NBI heating on the FI distribution.
As shown below, the recently upgraded NCU provides helpful insight into the activity and behaviour of fast ions, and the results from the recent campaign are shown here.

First MAST-U results

The NCU was commissioned half-way through the first MAST-U campaign MU01 on the 24th August 2021 and data for ~200 pulses was collected.

Here are presented selected results showing a variety of plasma scenarios, containing MHD instabilities such as Sawteeth and TAEs, and a comparison of the FI distribution with on- vs off-axis NBI heating to observe the effect on the FI density profile.

Other results display the effect of plasma rotation on fast ion confinement, and comparisons of the NCU count rates with the predictions of TRANSP and the measurements from the Fission Chamber (FC), the other neutron diagnostic on MAST-U.

TRANSP simulations were run on selected pulses to validate that the NCU works as expected, and general agreement is found between them.

The NCU

The Neutron Camera Upgrade, detailed in [1], detects the 2.45MeV neutrons produced by a branch of D-D reactions, along a set of six equatorial lines of sight. Since FIs are connected with the fusion reactions, the NCU indirectly observes the FI population and is thus a FI diagnostic.
Since Beam-Thermal reactions are dominant in MAST-U, the NCU is well-suited to the study of confined FIs.
The NCU consists of a shield with channels which act as collimators, placed before scintillating detectors, one collimator and one detector for each line of sight.

It features:
-- a time resolution of 1 ms
-- a spatial resolution of 10 cm
-- 0.5-1.2 impact parameter (perpendicular distance from the Line of Sight to the central column) range.

The total count rate is a combination of neutrons and gamma rays originating within the lines of sight, and also scattered neutrons; Pulse Shape Discrimination is employed during analysis to distinguish between gamma rays and neutrons, while Monte Carlo codes compute the scattered neutron component (**MCNP**), the scintillator response function (**NRESP**), and the solid angle of each line of sight (**LINE2**, plus an analytical model with excellent agreement).

The collimating shield reduces the scattered neutron contribution to the count rate by moderating incident neutrons; as these are frequently captured and gamma rays are emitted, a lead shield is also used around the detectors. One major improvement of the NCU over the prototype, shown in [2], is a reduction in the number of gamma rays reaching the scintillators.

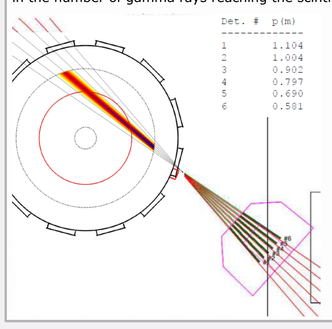

Left: A cross-sectional diagram of the NCU (purple box in the lower-right) seen from above in position around the MAST-U vessel, with the lines of sight denoted and the solid angle for one line of sight marked in colour; darker regions denote those which contribute more to the solid angle. The key shows the impact parameter of each line of sight in the NCU reference position.

Right: A CAD model cross section of the NCU around the MAST-U vessel, with the NBI beams shown in green and the NCU lines of sight in blue, with the full solid angle shown for the outer two lines of sight.

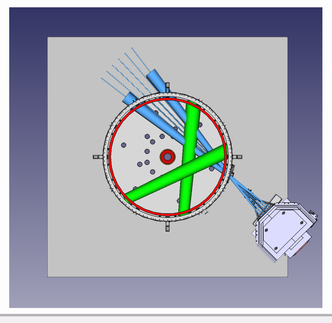

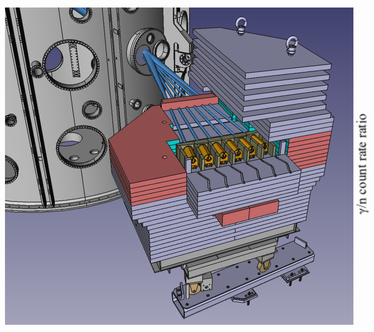

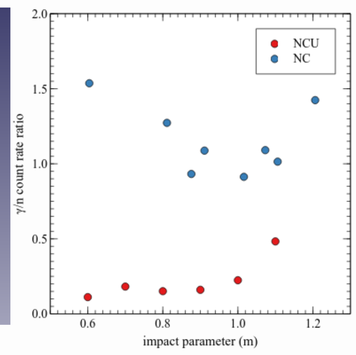

Top-left: A cutaway CAD model of the NCU in position around the MAST-U vessel, showing the six lines of sight (DARK BLUE) and the scintillators (DARK ORANGE).

Top-right: A comparison of the gamma ray to neutron ratio for the Neutron Camera (BLUE) and its upgrade, the NCU (ORANGE). The NCU has a much lower ratio, indicating better shielding of gamma rays.

MHD Instabilities: Sawteeth

-- **Sawteeth** are clearly visible as sudden crashes in the neutron count rate in both the NCU and FC data.

-- The neutron count rate profile can be seen in the measurements along the six lines of sight; it is peaked around the magnetic axis and flattens after a sawtooth crash, indicating the redistribution of fast ions from the centre.

-- TRANSP simulations of the pulse agree qualitatively concerning the FI redistribution, but agree less concerning the total neutron count rates.

-- Notably, when both on- and off- axis beams are in operation, the sawtooth peaks are larger and less frequent compared with when only one beam is running, as is seen in the time trace for pulse 45101, in which the off-axis NBI is only active for half the duration of the on-axis beam.

Below: NCU count rates for each impact parameter. The rates grow larger towards the plasma core and are consistently 50-100% larger near the centre compared with the edge.

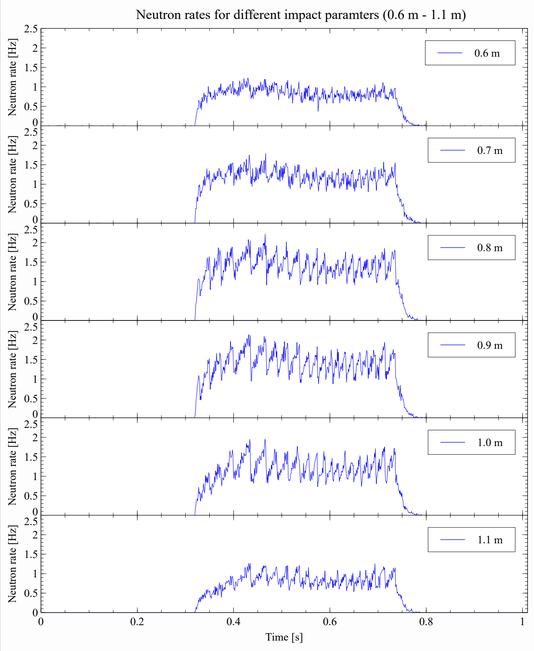

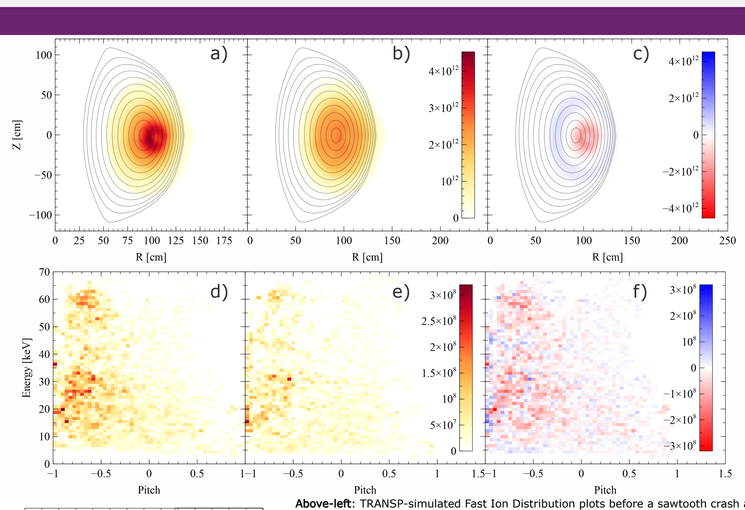

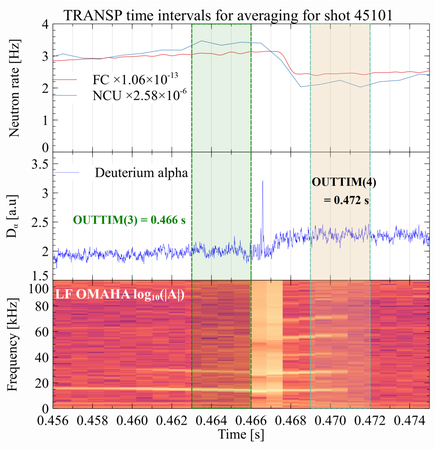

Right: The global timetrace for MAST-U pulse 45101. The off-axis (SW) NBI beam is active for around 200 ms, during which time the sawtooth peaks are larger and are less frequent than which occur when only the on-axis (SS) beam is active.

Below-right: The neutron count rate profile as a function of time. The impact parameter is plotted along the vertical axis. Repeated crashes can be seen at times when the profile is extremely red in the centre (i.e high count rates) followed by a green/blue profile (i.e low count rates).

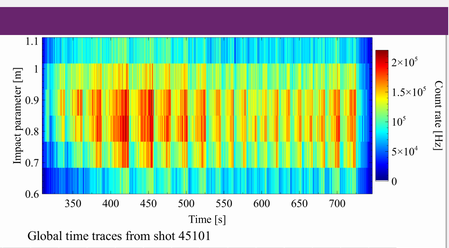

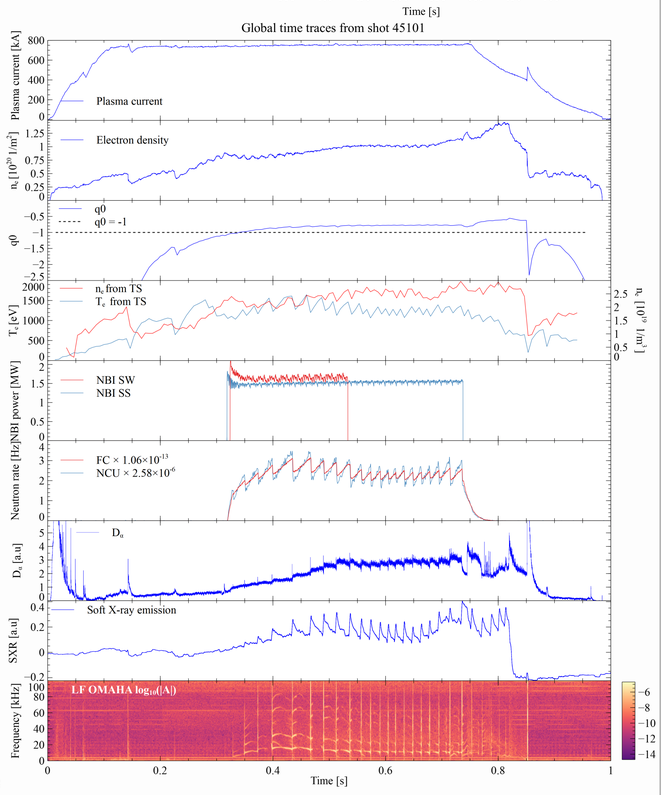

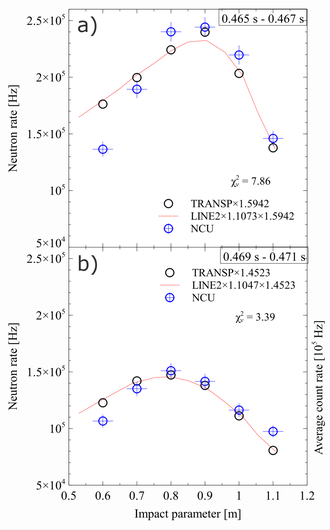

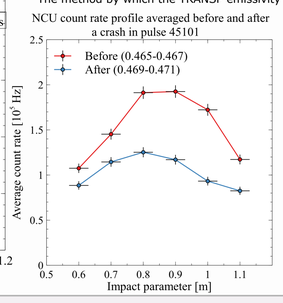

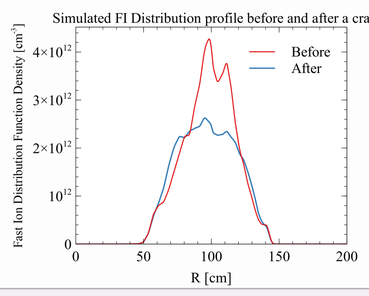

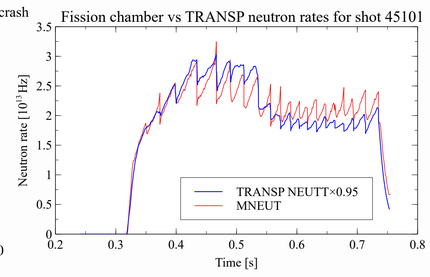

Above-left: TRANSP-simulated Fast Ion Distribution plots before a sawtooth crash at 0.466 s (a) and after at 0.472 s (b), and the change (c) in the distribution, with red indicating loss and blue indicating gain. The centre has lost FIs while regions closer to the edge have gained them, indicating that the sawtooth has flattened the FI distribution by ejecting FIs from the core. The change is visible in the corresponding on-axis pitch-energy plots for the FIs (d,e,f); the distribution, which has a dense region at the top from the NBI, reduces almost uniformly from before to after the crash, indicated by the largely red appearance of plot (f).

Above-right: The NCU, FC, Dα timetraces and OMAHA spectrogram zoomed in on the sawtooth crash corresponding to the above. The dashed lines mark the times up to which values are averaged for 3 ms, before and after the crash.

Below-right: The TRANSP-simulated neutron count rate timetrace vs that measured by the FC, both scaled. The simulation used the Kadomtsev model with particle mixing.

Below-middle: TRANSP-simulated FI distribution function density profiles before and after the same crash.

Below-left: NCU count rate profiles before and after a sawtooth crash.

Left: The TRANSP-simulated neutron rate radial profile together with NCU measurements averaged over 2 seconds before (a) a sawtooth crash and after (b). "LINE2" denotes the neutron rate predicted using solid angles calculated by the *LINE2* Monte Carlo code. The y-axis has the same scale in both. The simulated profile agrees qualitatively with the NCU, and both show a significant flattening after the crash.
The method by which the TRANSP emissivity in the poloidal cross-section is converted into a simulated NCU emissivity profile is detailed in [6].

On-axis vs off-axis NBI

On-axis and off-axis NBI beams are present on MAST-U because experiments on MAST indicated possible improvements in FI confinement in the off-axis scenario [3], attributed to the reduction in the spatial gradient of the FI distribution, reducing the growth rate of energetic particle modes (EPMs) [4].

--The measured distributions of fast ions in MAST-U in two scenarios, on-axis only, and off-axis only, are shown.

--With only off-axis NBI, the neutron rate and thus the FI distribution is flatter and is spread out, while in the on-axis case the density profile is clearly peaked centrally, as predicted [5].

--The shape of the distributions is visible in the NCU neutron rate profiles, and are compared with the TRANSP simulations to show good agreement.

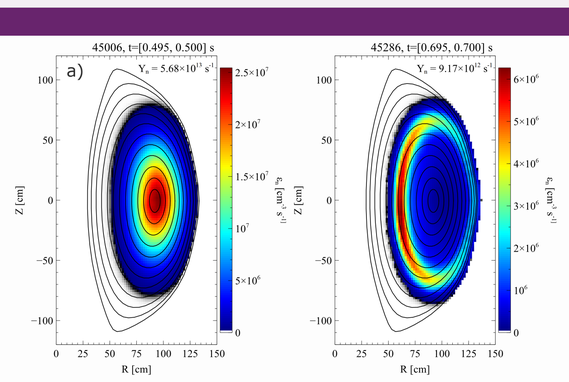

Above: The TRANSP-simulated neutron emissivity for MAST-U pulses with on-axis NBI heating (a) and off-axis (b). Red indicates larger emissivity. In the on-axis case, the majority of the emissivity is on-axis, and in the off-axis case the emissivity is shifted inwards and appears more spread out over the flux surfaces, and the on-axis emissivity is a factor of 20 lower.

Below: Corresponding NCU neutron count rate profiles compared with those predicted by TRANSP; good qualitative agreement is found. Scaling factors have been used to ensure that the qualitative agreement can be seen even if the absolute scale features some discrepancy. "LINE2" denotes the neutron rate predicted using solid angles calculated by the *LINE2* Monte Carlo code.

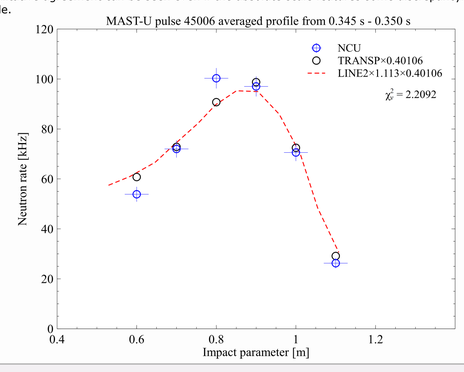

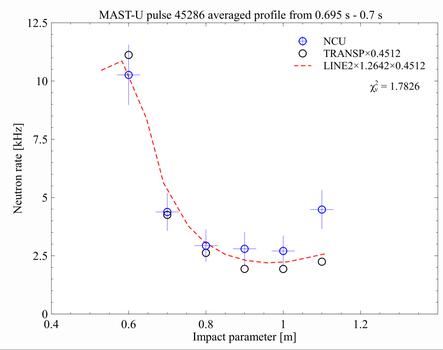

TAEs

Toroidal Alfvén Eigenmodes (TAEs) can be seen in MAST-U pulses immediately after the introduction of on-axis NBI heating. They can also be observed with the NCU where the neutron rate profile shows a change in the core, indicating a redistribution of fast ions.

Below: panel (a) TAEs evidence in the OMAHA pick-up coil signal and spectrogram; panel (b) FI redistribution due to the TAEs in the time interval indicated by the colored regions in panel (a).

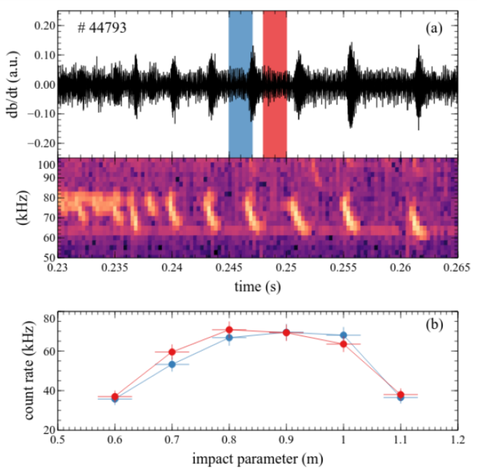

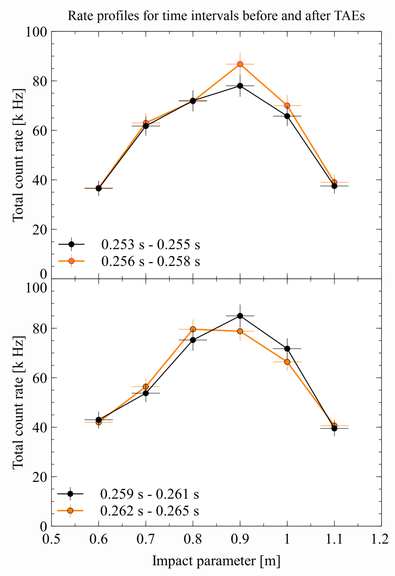

Above: NCU count rate peaks before and after two different peaks later on in pulse 44793. In A1) the height of the peak increases and in A2) it decreases, both by around 10%.

Fishbones

Fishbones (FBs) can be seen occasionally in MAST-U pulses, and are identifiable by sharp downward chirps in frequency in the OMAHA spectra, and lead to large FI losses.
The neutron count rate profile reduces almost uniformly across the profile, indicating that the FIs are actually lost and not only redistributed.

Below: panel (a) FBs evidence in the OMAHA pick-up coil signal and spectrogram; panel (b) FI losses due to the FB in the time interval indicated by the colored regions in panel (a).

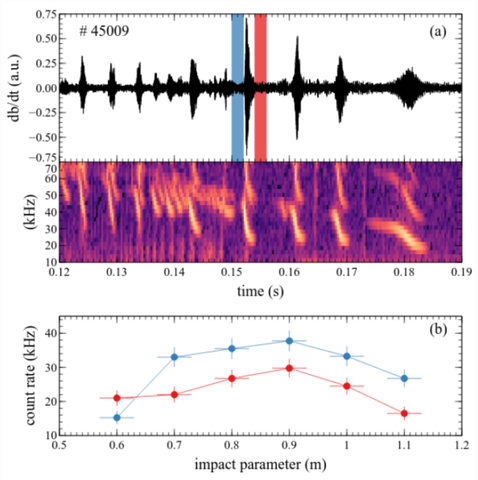

Plasma rotation

Plasma rotation is correlated with FI confinement.
The correlation can be seen in the neutron rates by comparing the predictions of TRANSP against the FC, as a scaling factor is required to match the neutron rates when rotation is present.

Top-right: a low-frequency OMAHA spectrogram for MAST-U pulse 44863 (top), and CHERS data for the same pulse (bottom), in which the colormap corresponds to the velocity.

Bottom-Right: The neutron count rates measured by the fission chamber (MNEUT) and simulated by TRANSP (NEUTT). Initially there is qualitative agreement, but the two diverge significantly after the plasma rotation slows, indicating a significant loss of FIs.

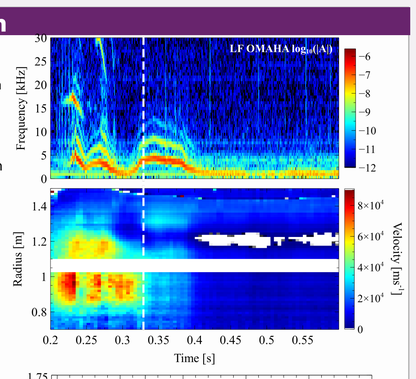

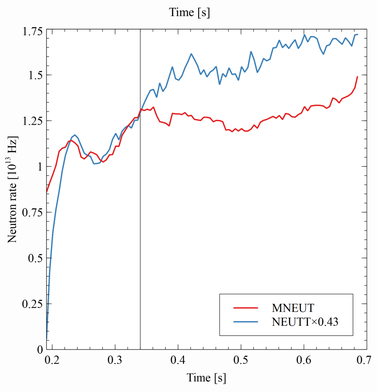

Count rate comparisons with FC

NCU and FC
--As the NCU and the FC are both neutron diagnostics, there should be qualitative agreement between them.
--The NCU is a diagnostic in the equatorial plane, so an absolute agreement with the FC which detects neutrons emitted globally from the entire plasma is not expected.
--The measured data shows that the count rates detected by the NCU are on the order of 10^6 times lower than the FC.
--The shape of the time traces are consistent, showing good qualitative agreement.

TRANSP and FC
--TRANSP allows values of anomalous fast ion diffusion (AFID) to be set manually to account for MHD activity ad hoc.
--TRANSP and the FC agree if AFID is set appropriately.
--The TRANSP neutron rates are scaled by a factor of around 0.6; its origin is likely linked to the guiding centre approximation used in NUBEAM [7] not being exactly applicable to spherical tokamaks, and a similar scale factor was required on MAST [8].

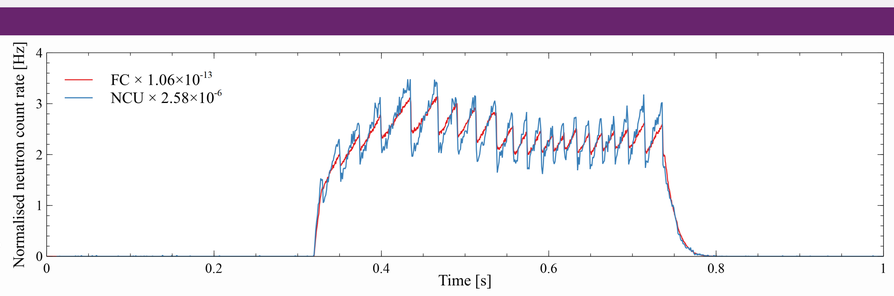

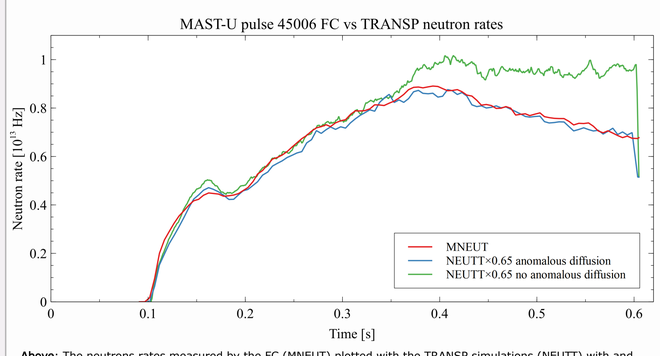

Above: The neutrons rates measured by the FC (MNEUT) plotted with the TRANSP simulations (NEUTT) with and without anomalous fast ion diffusion rates manually specified. Without them, the count rates diverge significantly after around 360 ms, just after an increase in MHD activity seen in the 10kHz region in the OMAHA trace.

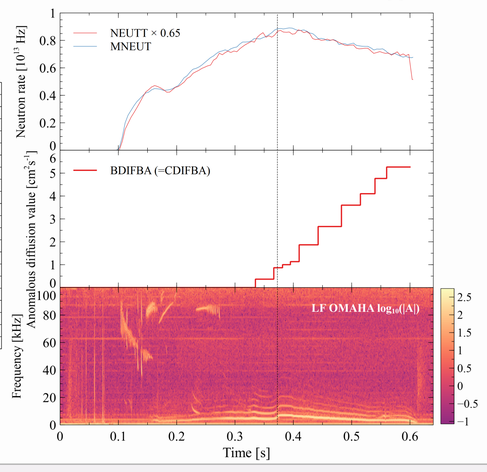

Above: The total neutron count rate for both the NCU and the FC during pulse 45101. There is qualitative agreement between the two instruments, except that the NCU sees sawteeth of larger relative amplitude due to the different regions of the plasma observed.

Right: Neutrons rates measured by the FC (MNEUT) plotted with TRANSP-simulated ones (NEUTT) for different NBI parameters for MAST-U pulses 45006 (a, on-axis NBI) and 45083 (b, off-axis NBI); scaling the on-axis beam power and changing the beam energy fractions produces simulations with closer agreement with those measured by the FC.

Left: Time traces for pulse 45006. (a) Neutron rates measured by the FC and simulated with TRANSP, with AFID values (BDIFBA and CDIFBA) chosen to account for the MHD activity present in the middle of the pulse. (b): AFID values vs time. (c): The spectrogram of low frequency OMAHA coils; a long MHD mode can be seen starting around 150 ms, increasing suddenly around 375 ms, and slowly decaying until the end of the pulse.

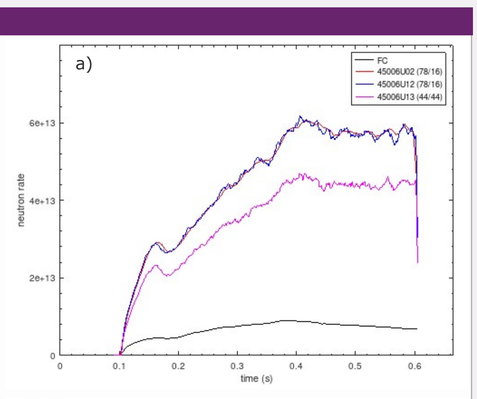

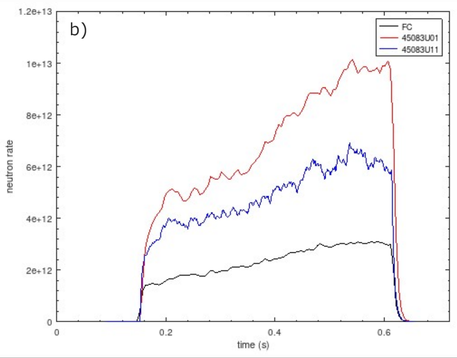

Conclusions

--The NCU is successfully performing according to its specifications.
--The profiles measured by the NCU are consistent with simulations and other FI diagnostics.
--Absolute agreement with simulation and other diagnostics is under investigation.
--The presented results confirm the rich nature of FI dynamics in MAST-U and will contribute to the development of improved operating scenarios and of dedicated FI experiments in the next MAST-U experimental campaign. Modelling of the FI redistribution and losses will be carried out in a follow up study within the framework of the reduced transport model.

Acknowledgements

This work is funded by the United Kingdom Engineering and Physical Sciences Research Council.
This work has been carried out within the framework of the EUROfusion Consortium, funded by the European Union via the Euratom Research and Training Programme (Grant Agreement No 101052200 — EUROfusion). Views and opinions expressed are however those of the author(s) only and do not necessarily reflect those of the European Union or the European Commission. Neither the European Union nor the European Commission can be held responsible for them. We would like to thank our colleagues from MAST.

References

[1] Cecconello M. et al. Review of Scientific Instruments 89 10I110 (2018)
[2] Cecconello M. et al. Nuclear Instruments and Methods in Physics Research A 753 (2014) 72–83
[3] Turnyanskiy M. et al. Nuclear Fusion 53 053016 (2013)
[4] McClements K. G. and Fredrickson E. D. Plasma Physics and Controlled Fusion 59 053001(2017)
[5] Morris A. W. et al. IEEE Trans. Plasma Sci. 42 402 (2014)
[6] Klimek I. et al. Nuclear Fusion 55 023003 (2015)
[7] Sperduti A. et al. Nuclear Fusion 61 016028 (2021)
[8] Cecconello M. et al. Nuclear Fusion 59 016006 (2019)